ADVANCED MATERIALS
www.advmat.de

Reconfigurable Optically Induced Quasicrystallographic Three-Dimensional Complex Nonlinear Photonic Lattice Structures

By *Jolly Xavier, Martin Boguslawski, Patrick Rose, Joby Joseph,* and *Cornelia Denz**

Quasicrystals (QCs) are materials that possess a long-range order with defined diffraction patterns, but lack the characteristic translational periodicity of crystals.[1] From the discovery of the non-crystallographic icosahedral quasiperiodic symmetry found in Al_6Mn in 1984,[2] the distinct properties of quasicrystallographic structures attracted a great deal of interest in different realms of science in recent years.[3] Another field of technological interest in the recent past is that of photonic crystals (PCs), the structured materials with a translational periodic modulation of the refractive index. Merging these two fields, a new class of material structures called photonic quasicrystals (PQCs) has drawn the attention of researchers stemming from a cumulative effect from both fields.[4,5] This is mainly due to the fact that the higher rotational symmetry of QCs leads to more isotropic and complete photonic bandgaps (PBGs) even in materials with a low refractive index contrast.[6,7] However, as in the case of PCs, the fabrication of 3D PQCs is much more involved in comparison to 2D PQCs and remains a real challenge today. Moreover, many of the conventional methods become technically either unsuitable or extremely complicated for the fabrication of 3D PQCs. Therefore, the fabrication and optimization of higher rotational symmetry 3D PQCs demand an approach that is flexible as well as reconfigurable. The purpose of the present Communication is dual fold. On the one hand, we demonstrate for the first time the generation of well-defined reconfigurable 3D quasi-crystallographic photorefractive nonlinear photonic structures with various rotational symmetries, which are experimentally realized in an externally biased cerium doped strontium barium niobate (SBN:Ce) photorefractive material as the nonlinear optical material of choice. These complex structures are envisaged to form a reconfigurable platform to investigate advanced nonlinear light–matter interaction in higher spatial dimensions with various rotational symmetries. On the other hand, we present a generalized versatile experimental approach for the fabrication of complex 3D axial PQCs with higher order rotational symmetry and variants of complex 3D structures similar to those having icosahedral symmetry, using a real-time reconfigurable holographic technique. It involves a programmable spatial light modulator (SLM)-assisted single step optical induction approach based on computer-engineered optical phase patterns. It is also important to note that the versatility of the experimental approach, we present, is not limited to photorefractive materials alone. It can be easily well adapted to various photosensitive materials as per the application requirement in the diverse fields of material science.

Among various photosensitive materials, reconfigurable nonlinear photonic lattices can be easily generated by means of a so-called optical induction technique[8–11] at very low power levels (~ micro watts) in a photorefractive material, exploiting the wavelength sensitivity of these materials.[8–13] The process of refractive index modulation, which leads to photonic lattice formation in such a medium is caused by a two-step process out of the incident light intensity distribution. Under the influence of an externally applied electric field, the incident light intensity distribution causes a charge carrier redistribution that results in a macroscopic space charge field in the photorefractive material. This, in turn, leads to a space-dependent refractive index modulation via the electro-optic effect thereby representing a nonlinear optical effect of third order that creates the refractive index modulation out of the incident intensity distribution.[8] Apart from the possibility of permanent fixing of the generated structures in a photorefractive crystal,[14] the recorded structure is reconfigurable: it can also be erased by the flush of white light so that new patterns could be again recorded in these materials. Therefore, photorefractive materials are ideal materials for reconfigurable PQC generation either to optimize the required photonic structure on the one hand or to be used as a reconfigurable platform to investigate novel nonlinear wave dynamics. From the optical properties point of view, the photonic lattices formed in SBN:Ce show both polarization as well as orientation anisotropy.[12,13] In order to obtain refractive index modulated structures that mimic the intensity pattern, o-polarized writing beams are used causing a low modulation due to the appropriate electro-optic coefficient addressed. For the case of using e-polarized writing beams, as the relevant electro-optic coefficient is much higher, a strongly nonlinear refractive index modulation can be obtained for the fabricated lattices.[13] Moreover, as maximum refractive index modulation is induced in the direction parallel to the crystal *c* axis, there exists also orientation anisotropy in SBN:Ce.

[*] Prof. C. Denz, J. Xavier, M. Boguslawski, P. Rose
Institut für Angewandte Physik and Center for Nonlinear Science
Westfälische Wilhelms-Universität Münster
Corrensstr. 2–4, Münster 48149 (Germany)
E-mail: denz@uni-muenster.de
J. Xavier, Dr. J. Joseph
Photonics Group, Department of Physics,
Indian Institute of Technology Delhi
Hauz Khas, New Delhi 110016 (India)

DOI: 10.1002/adma.200901792

Using the optical induction technique, 1D and 2D PC structures have been realized in photorefractive materials.[8–11] Although the refractive index modulation in a photorefractive material is low ($\sim 10^{-4}$), bandgaps appear in these materials due to the effect of Bragg scattering of eigenwaves – Bloch waves – of the induced lattice propagating at small angles. They can be found as solutions of the nonlinear Schrödinger equation describing light propagation in these photonic lattices.[8,9] The existence of 1D as well as 2D photonic bandgaps has been demonstrated,[8,9] enabling to realize a wealth of nonlinear optical phenomena in discrete lattice systems as the formation of discrete optical solitons, tunnelling effects, or quantum effects as Anderson localization.[8] Recently, we experimentally investigated 3D periodic structures in photorefractive medium.[11]

By its simplicity and flexibility in parameter control, holographic lithography-based technique has emerged as one of the highly promising approaches for scalable 3D PC templates or structures in large area with sub-micrometer periodicity.[4] In this approach, a refractive index modulation in the recording material is induced by means of interference of incident lattice-forming light beams. It has been theoretically proposed that PC structures belonging to all fourteen 3D Bravais lattices could be fabricated either by the interference of multiple beams or by the multiple exposure of two beam interference.[15,16] As implemented in the case of periodic PC structures, recently, various optical induction-based fabrication approaches have been adapted to fabricate 2D[17–19] as well as 3D[20–25] PQCs in different photosensitive materials. In three dimensions, both 3D axial PQCs as well as variants of icosahedral structures have been investigated.[20–25] In the case of 3D axial PQCs there is quasiperiodicity in x–y plane while the periodicity remained along z axis.[21,25] However, in mostly reported fabrication of 3D PQCs, either the lattice-forming light wavelength is to be varied or optical components/setup is to be manipulated with high precision in order to realize 3D PQCs with variable lattice geometry or periodicity between similar structures.[21–25] Moreover, these approaches mainly involve single or multiple exposure of interfering beams coupled with precisely designed fixed discrete optical elements.

In our approach, n-fold 3D axial PQCs are fabricated by means of $n+1$ interfering beams, where a central beam is surrounded by angularly displaced side beams. For the variants of 3D quasiperiodic complex structures similar to icosahedral QCs,[22–24] the beam geometry with respect to the central beam is designed such that the resultant interference pattern induces the 3D PQC structure. The lattice-forming beams necessary to create the irradiation profile for a particular 3D PQC are generated by a computer-engineered phase pattern, representing the phase information extracted from the overall complex amplitude of the calculated structure. This phase pattern is sent to a programmable phase-only SLM, and it spatially modulates a plane wave incident on the SLM. By modifying the phase-engineered pattern, different lattice periodicities between similar structures and structural variations can easily be attained. Moreover, typically no additional optical components or manipulation of the experimental setup, like rotating the recording medium, is involved during the process of fabrication. This gives rise to the flexibility of generating reconfigurable 3D PQC structures in real time.

The irradiance profile of $(n+1)$ plane wave-interference is given by,

$$\mathbf{I}(\mathbf{r}) = \sum_{j=1}^{n+1} \left|\mathbf{E}_j\right|^2 + \sum_{i\neq j}^{n+1} \mathbf{E}_i \cdot \mathbf{E}_j \exp[i(\mathbf{k}_i - \mathbf{k}_j)\cdot \mathbf{r} + i(\psi_i - \psi_j)] \tag{1}$$

where $\mathbf{E}_i$, $\mathbf{k}_i$, $\mathbf{r}$ and ψ_i are respectively complex amplitudes, wave vectors, position vector and the initial phase of the interfering beams. The interfering beams are linearly polarized in the direction relative to the crystal c axis of the recording photorefractive medium oriented as per the lattice orientation requirement. The central beam is incident normal to the x–y plane of the recording medium. For an n-fold symmetry 3D axial PQC structure, the wave vectors of the side beams could be given by,

$$\mathbf{k}_m = k\left(\cos\frac{2\pi(m-1)}{n}\sin\theta_i, \sin\frac{2\pi(m-1)}{n}\sin\theta_i, \cos\theta_i\right) \tag{2}$$

where m is from 1 to n, $k = 2\pi n_r/\lambda$ and λ is the wavelength. n_r is the refractive index of the recording medium. For SBN:60, n_e and

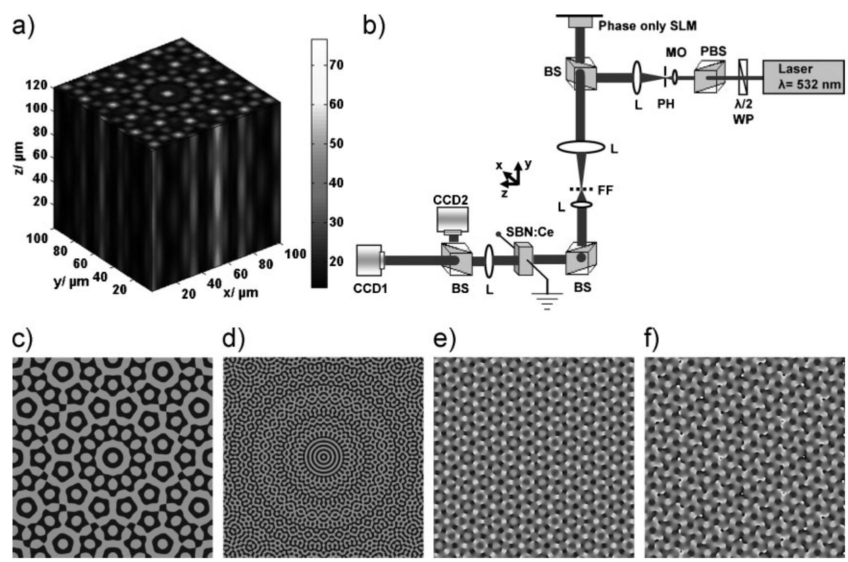

Figure 1. a) Simulated interference intensity distribution for 12-fold 3D axial PQC. b) Schematic representation of the experimental setup for the fabrication and analysis of 3D PQCs in an externally biased SBN:Ce photorefractive crystal. WP: wave plate, PBS: polarizing beam splitter, MO: microscope objective, PH: pinhole, L: lens, BS: beam splitter, FF: Fourier filter. c)–f) Computer engineered phase patterns for generating 3D PQCs: c, d) for generating variant of 3D axial PQC with12-fold and 32-fold rotational symmetry, e, f) for generating 3D icosahedral PQC and complex 3D PQCs, respectively.

n_o, the unperturbed refractive indices experienced by extraordinarily polarized (e-polarized) wave and ordinarily polarized (o-polarized) wave at $\lambda \sim 532$ nm are, respectively, 2.324 and 2.354.[26,27] θ_i is the angle between the central beam and the side beams. Figure 1a shows an example of simulated three-dimensional intensity distribution of the interference pattern for a 12-fold rotational symmetry 3D axial PQC using $\theta_i = 15°$. The related phase-engineered pattern is computed from the total phase ($\varphi_i(x,y)$) of the over all complex amplitude resulting from the superposition of intended all lattice forming beams, $\mathbf{E}(\mathbf{x},\mathbf{y}) = \mathbf{E}_0 \sum_{i=1}^{n+1} \exp[i\phi_i(\mathbf{x},\mathbf{y})]$. The computed phase patterns are sent to SLM in order to spatially modulate the incident plane wave. The phase patterns for different lattice beam geometries are given in Figure 1c–f.

As QC structures are envisaged to show novel wave propagation dynamics and guiding properties, 2D QCs have been investigated in photorefractive crystals.[28] Here, we experimentally explore the fabrication of 3D PQCs with higher-order rotational symmetry, which are not yet realized in photorefractive material. Cerium doped $Sr_{0.60}Ba_{0.40}Nb_2O_6$ (SBN:Ce) photorefractive crystal is used in our experiments.[26,27] Various 3D axial PQCs, belonging to odd as well as even order rotational symmetries, are experimentally generated in an externally biased SBN:Ce. Figure 1b shows the schematic view of the experimental setup. For a 32-fold symmetry 3D axial PQC, a single-step interference of 33 coherent beams is realized, which is almost impossible by conventional multiple-beam interference approach. Even the 3D axial PQCs with further higher-order rotational symmetry could be easily realized. Figure 2 shows the images of x–y and x–z planes of various 3D PQCs fabricated in an externally biased SBN:Ce photorefractive medium. An e-polarized broad plane wave is guided through the generated lattice in order to qualitatively image the fabricated structure. The effect of orientation anisotropy also affects the generated pattern in SBN:Ce, as the refractive index modulation induced in the direction perpendicular to the crystal c axis is minimum. Figure 3 gives different variants of fabricated 3D axial PQCs with 12-fold rotational symmetry. Another flexibility of the approach to vary the initial phase of the individual beams leading to variant of a particular structure with same rotational symmetry is given in Figure 3c. For the fabrication of this variant of 12-fold symmetry PQC structure, the alternating lattice-forming side beams have an additional initial phase ψ_i of 0 and π respectively. The fabricated 3D PQC of 12-fold symmetry with reduced distance between similar structures is shown in Figure 3d, which is realized by appropriately designing the periodicity of the phase pattern. The far-field diffraction patterns of various 3D axial PQCs clearly depict their characteristic higher-order rotational symmetry, which is in a way 'forbidden' in terms of crystallographic periodicity.

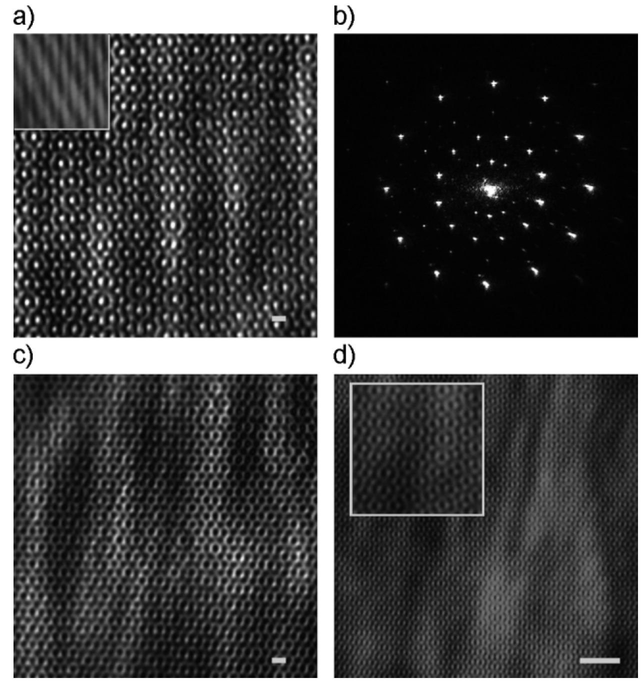

Figure 3. Recorded images of 12-fold rotational symmetry 3D axial PQC fabricated in SBN:Ce. a) x–y plane of the photonic lattice, x–z plane is given in the inset. b) far-field diffraction pattern. c) x–y plane of a variant of 12-fold rotational symmetry 3D axial PQC, fabricated with lattice forming beams with an additional π initial phase for alternating interfering side beams. d) 12-fold symmetry 3D PQC fabricated with reduced distance between the similar structures in comparison to (a). The inset in (d) projects a part of the image being enlarged. All scale bars = 10 μm.

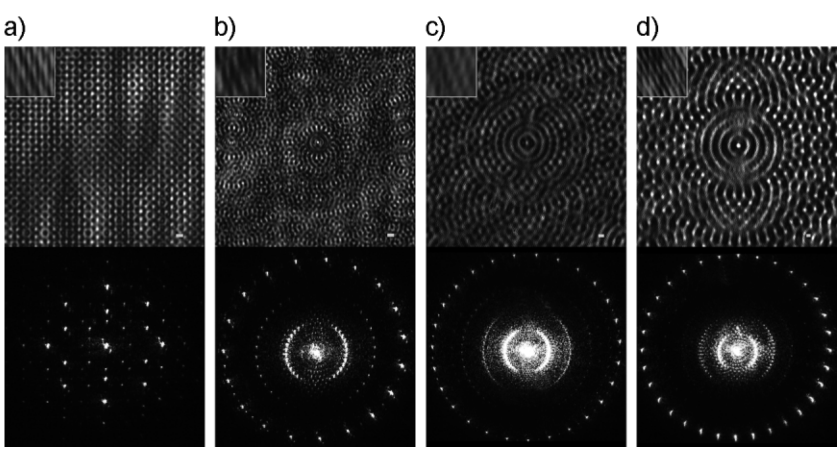

Figure 2. Upper row: Recorded images of x–y plane of 3D axial PQCs being fabricated in an externally biased SBN:Ce photorefractive crystal. 3D axial PQCs with rotational symmetry: a) 8-fold, b) 19-fold, c) 27-fold, and d) 32-fold. The recorded images of a portion of the x–z plane of the structures, containing a region near to the propagation axis, are shown in the inset. Lower row: Far field diffraction patterns belonging to the structures in the upper row. All scale bars = 10 μm.

For a variant of 3D icosahedral PQC,[22,24] we computed the phase pattern (Fig. 1e) and generated the lattice-forming beams such that 5 side beams, with their wave vectors lying 72° apart from each other in the projected plane, interfered with two counter-propagating central beams along the z axis. The 10-fold symmetry of 5-fold axis is clearly observed in the image of the x–y plane of the generated structures

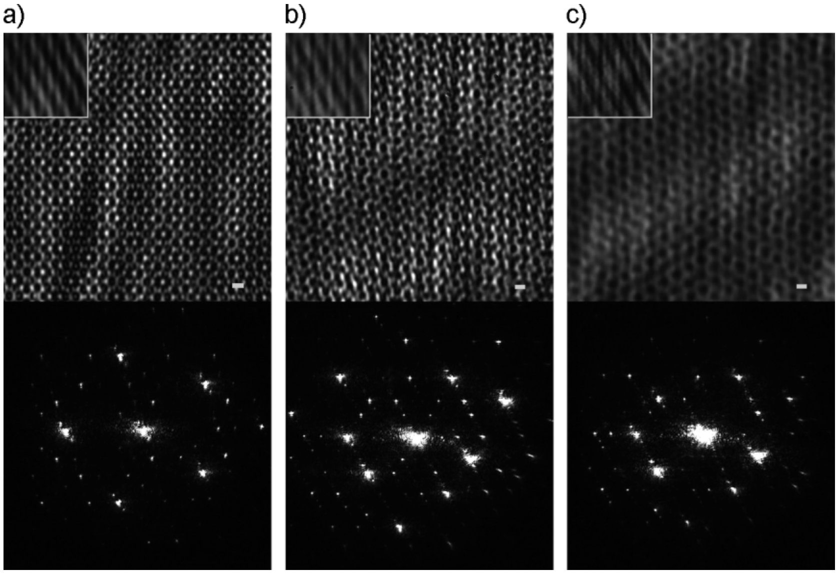

Figure 4. Recorded images of 3D icosahedral and complex 3D PQCs fabricated in SBN:Ce. a) *x–y* plane of a variant of 3D icosahedral PQC. b) and c) *x–y* planes of complex 3D PQCs using a specially designed seven beam geometry, where (b) is generated by single exposure and (c) by double exposure. Recorded image of the *x–z* plane of the generated 3D PQCs is given in the inset. Far field diffraction patterns are given below the structures. All scale bars = 10 μm.

recorded by the guided wave intensity distribution as shown in Figure 4a (the image of the *x–z* plane is given in the inset of Fig. 4a). Another flexibility of the present approach is the single-step generation of non-coplanar lattice forming beams belonging to complex 3D photonic lattice geometry. To demonstrate this by means of a phase-engineered pattern (Fig. 1f), a complex beam geometry consisting of seven beams (one central and six side beams) is designed. The six side beams could be considered as belonging to two sets of three beams each, a_i and b_i, where $i = 1$–3, forming an angle θ_{ai}, and θ_{bi} with the central beam along the *z* axis, respectively. On the projected plane, the three wave vectors of each set are separated from each other by an angle of 120°. The wave vectors of a_i are angularly displaced from those of b_i by an angle γ in the same plane. As an example, we show two variants of complex 3D PQCs fabricated in SBN:Ce using the values $\gamma = 37.7°$, $\theta_{ai} = 16.5°$, and $\theta_{bi} = 23.6°$. The seven lattice-forming beams are generated in a single step by appropriately computed phase patterns being sent to SLM. The first variant of the complex PQCs are formed in a single exposure involving interference of all seven beams. In the second case, two exposures are carried out without manipulating the experimental setup of recording medium. The first exposure is taken using the central beam and a_i side beams, followed by a second exposure in which only six side beams are involved while the central beam is blocked. The beams are chosen by means of a simple Fourier filter. The images of the photonic lattices of complex 3D PQCs and their respective far field diffraction patterns are given in Figure 4b and c.

In conclusion, we have presented a versatile approach for the fabrication of large area 3D PQC complex structures by a single step optical induction approach. By means of computer-engineered reconfigurable phase patterns, lattice-forming beams are generated to fabricate 3D PQCs belonging to various rotational symmetries. As a versatile experimental technique, these lattice-forming beams are generated by a programmable SLM-based approach. Moreover, variants of a number of structures with different shapes and periodicities between similar structures could be realized in real time. It is demonstrated that by this approach, different 3D axial PQCs and variant of 3D icosahedral QC as well as complex 3D PQCs can be fabricated with flexibility in parameter control. Using this fabrication approach, we have experimentally demonstrated well-defined reconfigurable nonlinear 3D quasicrystallographic complex structures in an externally biased SBN:Ce photorefractive crystal. The fabricated 3D PQC structures were analyzed by imaging the plane wave guided intensity distribution from different directions. Their respective far-field diffraction patterns were also imaged, verifying the defining higher-order rotational symmetry of generated PQCs. These complex photorefractive nonlinear 3D structures form a reconfigurable platform for the investigation of advanced nonlinear light-matter interactions such as spatio-temporal solitons, enhanced tunneling and mode localization, etc, in higher spatial dimensions.[8,9] These investigations would play a key role for nonlinear photonic device integration in new generation all optical active devices. Moreover, the presented real-time reconfigurable fabrication approach for scalable complex 3D PQCs could be very well adapted to different photosensitive materials pertaining to diverse fields of material science. This, in turn, paves a way for fabricating quasicrystallographic photonic templates for the realization of highly preferred complex PBG structures or advanced artificial complex material structures for promising potential applications like highly efficient flat-panel displays with customized angular emission.[29]

Experimental

Fabrication and Analysis of 3D PQCs in Externally Biased SBN:Ce: As shown in the schematic representation of the experimental setup given in Figure1b, a linearly polarized beam at $\lambda = 532$ nm wavelength is derived from a frequency doubled continuous wave Nd:YAG laser. The collimated wave is spatially phase modulated in order to generate the lattice-forming wave. This modulation is accomplished with the help of a high-resolution programmable phase-only SLM (Holoeye PLUTO-VIS, 1920 × 1080 pixels) by means of computer-engineered phase patterns, encoded in appropriate gray scale. The generated lattice-forming wave is imaged to the input face of a 5 mm long Cerium doped $Sr_{0.60}Ba_{0.40}Nb_2O_6$ (SBN:Ce) photorefractive crystal using a high numerical aperture telescope. We have used a demagnification of ~7 times. SBN:Ce is biased (along crystal c-axis) by an externally applied electric field of 1.5 kV cm^{-1}. Taking the beams all together, the power of the lattice-forming wave was measured to be in the range of 40–60 μW. For the lattice-forming beams, the intensity of the central beam is typically couple of times higher in comparison to an individual side beam. The exposure time was in the order of 60 to 90 s. Considering the dense Fourier spectrum of QCs [1] as well as the polarization anisotropy of SBN:Ce [13], in order to realize a non-distorted refractive index modulation, an o-polarized wave is used for the lattice formation. An e-polarized broad plane wave is used for the analysis of the fabricated structures exploiting the increased diffraction efficiency resulting from the large electro-optic effect in this polarization direction. In the case of 3D icosahedral PQC, the seventh beam propagating in the direction opposite to that of the central beam is formed using a high-reflectivity mirror kept close to SBN:Ce such that only the central beam is reflected back. The periodicity between similar structures in fabricated PQCs could be experimentally varied by means of demagnification optics as well as engineering the modulating phase pattern within the span of available pixel resolution of the SLM. The fabricated 3D PQCs were analyzed using two established experimental tools [10,23]. First, we imaged the guided intensity distribution of an e-polarized broad plane wave having a low light intensity ($\sim$1:10 in comparison to the lattice-forming wave) through the fabricated structures. To ensure 3D lattice formation, we imaged the structure from two perpendicular directions using CCD1 capturing the x–y as well as x–z planes of the fabricated 3D lattice. In order to image the x–z plane, the SBN:Ce was rotated by 90°. Secondly, the far-field diffraction patterns from the fabricated 3D PQCs were recorded using CCD2 kept at the Fourier plane of the output lens.

Acknowledgements

J. X. gratefully acknowledges support from German Academic Exchange Service (DAAD).

Received: May 28, 2009
Published online: September 14, 2009

[1] C. Janot, *Quasicrystals: A Primer*, Clarendon, Oxford **1994**.
[2] D. Shechtman, I. Blech, D. Gratias, J. W. Cahn, *Phys. Rev. Lett.* **1984**, *53*, 1951.
[3] J.-M. Dubois, *Mater. Sci. Eng. A* **2000**, *294*, 4.
[4] *Photonic Crystals: Advances in Design, Fabrication, and Characterization*, (Eds: K. Busch, S. Lölkes, R. B. Wehrspohn, H. Föll), Wiley-VCH, Weinheim, Germany **2004**.
[5] M. Peach, *Mater. Today* **2006**, *9*, 44.
[6] M. E. Zoorob, M. D. B. Charlton, G. J. Parker, J. J. Baumberg, M. C. Netti, *Nature* **2000**, *404*, 740.
[7] W. N. Man, M. Megens, P. J. Steinhardt, P. M. Chaikin, *Nature* **2005**, *436*, 993.
[8] F. Lederer, G. I. Stegeman, D. N. Christodoulides, G. Assanto, M. Segev, Y. Silberberg, *Phys. Rep.* **2008**, *463*, 1.
[9] D. N. Neshev, A. A. Sukhorukov, W. Krolikowski, Y. S. Kivshar, *J. Nonlinear Opt. Phys. Mater.* **2007**, *16*, 1.
[10] A. S. Desyatnikov, D. N. Neshev, Y. S. Kivshar, N. Sagemerten, D. Traeger, J. Jaegers, C. Denz, Y. V. Kartashov, *Opt. Lett.* **2005**, *30*, 869.
[11] C. Denz, B. Terhalle, D. Göries, P. Rose, J. Xavier, T. Richter, A. S. Desyatnikov, J. Imbrock, T. J. Alexander, D. N. Neshev, J. Joseph, F. Kaiser, W. Krolikowski, Y. S. Kivshar, *Proc. SPIE Int. Soc. Opt. Eng.* **2009**, *7354*, 735402.
[12] N. K. Efremidis, S. Sears, D. N. Christodoulides, J. W. Fleischer, M. Segev, *Phys. Rev. E* **2002**, *66*, 046602.
[13] B. Terhalle, A. S. Desyatnikov, C. Bersch, D. Traeger, L. Tang, J. Imbrock, Y. S. Kivshar, C. Denz, *Appl. Phys. B* **2007**, *86*, 399.
[14] J. J. Amodei, D. L. Staebler, *Appl. Phys. Lett.* **1971**, *18*, 540.
[15] L. Z. Cai, X. L. Yang, Y. R. Wang, *Opt. Lett.* **2002**, *27*, 900.
[16] A. Dwivedi, J. Xavier, J. Joseph, K. Singh, *Appl. Opt.* **2008**, *47*, 1973.
[17] X. Wang, C. Y. Ng, W. Y. Tam, C. T. Chan, P. Sheng, *Adv. Mater.* **2003**, *15*, 1526.
[18] M. Guo, Z. Xu, X. Wang, *Langmuir* **2008**, *24*, 2740.
[19] G. Zito, B. Piccirillo, E. Santamato, A. Marino, V. Tkachenko, G. Abbate, *Opt. Express* **2008**, *16*, 5164.
[20] A. Ledermann, L. Cademartiri, M. Hermatschweiler, C. Toninelli, G. A. Ozin, D. S. Wiersma, M. Wegener, G. Von Freymann, *Nat. Mater.* **2006**, *5*, 942.
[21] X. Wang, J. Xu, J. C. W. Lee, Y. K. Pang, W. Y. Tam, C. T. Chan, P. Sheng, *Appl. Phys. Lett.* **2006**, *88*, 051901.
[22] W. Y. Tam, *Appl. Phys. Lett.* **2006**, *89*, 251111.
[23] N. D. Lai, J. H. Lin, Y. Y. Huang, C. C. Hsu, *Opt. Express* **2006**, *14*, 10746.
[24] J. Xu, R. Ma, X. Wang, W. Y. Tam, *Opt. Express* **2007**, *15*, 4287.
[25] I. Bita, T. Choi, M. E. Walsh, H. I. Smith, E. L. Thomas, *Adv. Mater.* **2007**, *19*, 1403.
[26] *High Frequency Properties of Dielectric Crystals, Landolt–Boernstein – Group III Condensed Matter*, Vol. *30A*, (Ed: D. F. Nelson), Springer, Berlin **1996**, Sec. 5.3. 4.
[27] M. D. Ewbank, R. R. Neurgaonkar, W. K. Cory, J. Feinberg, *J. Appl. Phys.* **1987**, *62*, 374.
[28] B. Freedman, G. Bartal, M. Segev, R. Lifshitz, D. N. Christodoulides, J. W. Fleischer, *Nature* **2006**, *440*, 1166.
[29] F. Rahman, *Opt. Photonics News* **2009**, *20*, 24.

